Structure of laser-plasma-driven shock waves expanding in an ambient gas

V.G. Borodin, V.M. Komarov, S.V. Krasov, V.A. Malinov, V.M. Migel, N.V. Nikitin, V.N. Chernov, and A.V. Charukhchev

Scientific Research Institute for Complex Testing of Opto-Electronic Devices, Sosnovyi Bor, Leningrad Region

Received March 9, 2000

The structure of strong laser-plasma-driven shock waves expanding in a low-pressure ambient gas has been studied with the use of a multiframe interferometry. It was found that conical shock waves are generated along with spherical ones. At the late stages, conical shock waves appear as projections ahead of a spherical wave. It is shown that these projections are not directly connected with the hydrodynamic instability of spherical shock waves.

As a solid-state target in a low-pressure gas is exposed to laser radiation, plasma is formed, which acts on the ambient gas as a plasma piston and forms a strong ionizing shock wave in it. The studies of this effect are interesting because of the limited experimental data on strong shock waves, whose structure and dynamics differ from those of well-studied weak waves.[1] The practical significance of experimental studies is connected with the investigation and simulation of various processes needed, in particular, for development of the methods of diagnostics of plasma heated by high-power laser radiation.

Strong ionizing shock waves excited by high-power laser radiation were observed and studied by various methods. Some papers considered the problems of stability of shock waves. In Ref. 2 the behavior of the laser-induced plasma was studied depending on the ambient gas pressure. It was found that the shock-wave structure at the laser plasma and shock wave separated by a contact boundary arises at the pressure $p > 1$ mm Hg. In Ref. 3, it was shown that at the pressure $p = (1 - 5)$ mm Hg the front of the shock wave has a smooth quasispherical shape. Inhomogeneity and instability typically observed at pressures $10^{-1} < p < 1$ mm Hg do not arise. Stratification of radiation and inhomogeneity are observed behind the front of the shock wave in deep layers in the form of a cramp.

In Ref. 4 the initial stage of motion of a spherical shock wave formed in the residual gas under the effect of high-temperature laser plasma at $p = 16$ mm Hg was studied. Experiments were conducted with spherical glass and polysterene targets. As spherical targets were exposed to radiation, no instability in the dynamic of shock waves was observed.[4,5]

In Ref. 6 it was shown that a part of energy of laser plasma is lost at conversion into the energy of a shock wave because of the escape of ions from the high-energy tail of the Maxwell distribution. These ions leave plasma without interaction with the shock wave. Instability in dynamics of strong shock waves was studied in Ref. 7. Experiments were conducted using the laser beams with the power density of $(10^{12}–10^{14})$ W/cm^2 on the target surface. The pressure of the ambient gas was held higher than 1 mm Hg. In shadow pictures, the wave front regions that markedly project beyond the neighboring spherical part were observed. These regions of the shock wave, called aneurisms by Stamper and Ripin,[7] are indicative, in their opinion, of the instability in the dynamics of strong shock waves.

The following peculiarities connected with the appearance of aneurisms were found. In most cases they arise at the ambient gas pressure higher than 1 mm Hg and at late spread time (> 50 ns); aneurisms arise near the axis of the laser beam, but sometimes they occur at a significant distance from the axis; inhomogeneity of the intensity distribution in the laser beam does not play the main part in the formation of aneurisms.

In this paper, we studied peculiarities of formation of the shock wave structure under the exposure of a solid-state target to subnanosecond Nd laser pulse at the power density of $(8 \cdot 10^{13} - 8 \cdot 10^{16})$ W/cm^2. The experiments were conducted with the Progress laser system.[8] The optical arrangement of the experiment is shown in Fig. 1.

A high-power laser beam with the energy up to 20 J and pulse duration of 0.2 ns was formed in the amplification channel *1*. The mirrors *2* and *3* directed the beam into a chamber with the target *4*, and the objective *5* focused it onto the target *6*. The radiation reflected by the mirror *7* was converted in the nonlinear crystal *8* into the second harmonic. The second harmonic radiation with the energy of 20 mJ was focused by the mirror *9* and lens *10* into the cell *11* of an SRS-compressor filled with methane. The reflected 0.02-ns long pulse in the backward direction was formed due to SRS compression.[9] The energy density in the cross section of the beam of 8 mm in diameter was 15 mJ/cm^2, the wavelength of the Stokes radiation was 0.625 μm. A part of a beam came to the Sirks interferometer formed by the mirrors *12* and *13*, one of

0235-6880/00/05 448-04 $02.00

whose arms housed the object under study *14*. The interferometer was tuned to bands of finite width, whose localization plane was matched by the objective *15* with the plane of recording *16* (*16′*, *16″*). The element *17* is a splitter of images obtained at different moments in time. The time interval between the sensing pulses was formed at the delay line formed by the mirrors *20* and *21* and the lenses *22* and *23*. A part of radiation was directed by the elements *18* and *19* to the delay line. The elements *24* and *25* outputted two pulses delayed with respect to each other. The mirror *26* directed the sensing beams into the interferometer, and they were used for recording the object at a later time.

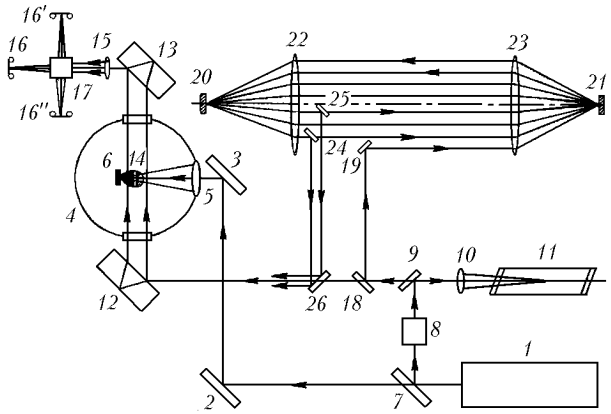

Fig. 1. Optical arrangement of the experiment.

Figure 2 shows the main elements of the shock wave structure, which can be observed in the interferograms (Fig. 4) discussed below in this paper. The laser beam of 120 mm in diameter was focused by the objective with the focal length of 170 mm, propagated in a cone bounded by the edge rays *1*, and concentrated on the surface of the target *2* at the point *3*. The diameter of the focal spot was 15 μm with regard for laser beam divergence. To determine the influence of the power density on the studied processes, in some experiments the beam was defocused while being focused at a point situated at some distance Δ above the target surface. The initial stage of formation of the shock wave corresponded to the time of recording $t = 5$ ns after the exposure of the target to the heating pulse (see Fig. 2*a*). The opaque zone consisting of two parts: spherical *4* (just above the focusing point *3*) and plane *5*, was adjacent to the surface. Between the spherical shock wave *6* and the opaque zone there were two gas layers: relatively homogeneous one *7* and strongly turbulized layer *8* adjacent to the trailing front of the spherical shock wave. The conic shock wave *9* propagates ahead of the front of the spherical shock wave, and the conic wave axis is directed along the radius originating at the focusing point *3*. Figure 2*b* shows the later stage of evolution of the shock wave corresponding to 65 ns after the target was exposed to the heating pulse; here *10* means the plane shock wave.

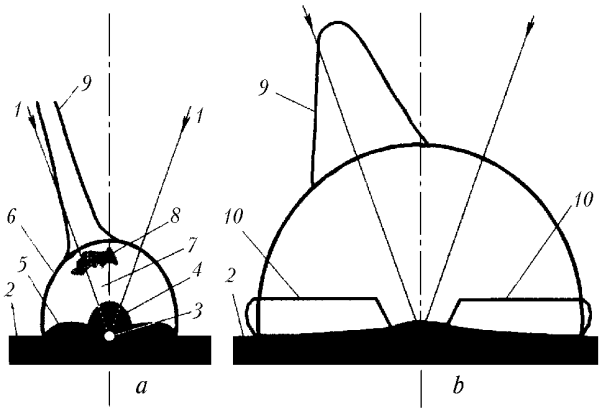

Fig. 2. Main elements of the structure of shock waves within 5 (*a*) and 65 ns (*b*) of action of heating pulse.

The following parameters were measured in the experiment: laser beam energy E_l, defocusing Δ, and the ambient gas pressure p. The power density q in the target illumination zone was calculated from these data with regard for the known size of the focal spot. The exposure time of every frame corresponded to the duration of the sensing pulse and was equal to 0.02 ns.

The shock waves were initiated by exposing a thick fluoroplastic target to a 0.2 ns long laser pulse. Experiments were conducted at different pressure p from 1 to 60 mm Hg. The results presented in Figs. 4*b–e* were obtained at the ambient air pressure of 15 mm Hg. However, all the peculiarities of the shock wave retain roughly from 5 to 40 mm Hg. At further increase in pressure at unchanged laser radiation power density, breakdown of the gas (Fig. 3) and formation of the cylindrical shock wave localized along the laser beam axis are observed (processes at $p > 40$ mm Hg are not considered in this paper). At $p \le 5$ mm Hg the phase shift produced by the shock wave in the sensing beam is close to the sensitivity limit of a single-pass interferometer, and shock waves can hardly be visualized.

A typical interferogram, which demonstrates the main peculiarities at the initial stage of formation of the shock wave, is shown in Fig. 4*a*. The result was obtained under the following experimental conditions: $E_l = 13$ J, $\Delta = 200$ μm, $p = 15$ mm Hg, $q = 8 \cdot 10^{13}$ W/cm^2, $t = 5$ ns. The hot spreading laser plasma leaving the spherical part of the opaque zone forms the spherical shock wave. The plane part of the opaque zone arises because of evaporation of a part of the target material due to propagation of a thermal wave from the zone illuminated by the laser beam. The conic shock wave with the axis directed along the radius originating at the beam focusing point *3* is clearly seen in the figure. At a later stage of the process (Fig. 4*b*), at $t = 65$ ns, the spherical opaque zone vanishes, and the plasma formed because of evaporation of the target material generates a plane shock wave propagating normally to the target surface.

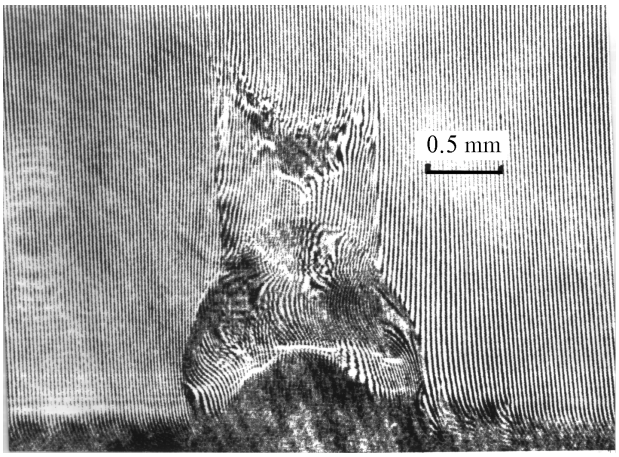

Fig. 3. The interferogram of a shock wave at the breakdown of the gas within 5 ns of action of the heating pulse on the target.

In this experiment, the conic shock wave arises inside the area occupied by the focused laser beam, and we can assume that it is connected with inhomogeneous heating of the ambient gas due to inhomogeneous distribution of radiation in the beam. However, as the power density increased up to $q = 8 \cdot 10^{16}$ W/cm^2 several such shock waves were observed, and some of them were outside the region occupied by the laser beam (as shown by a circle in Fig. 4*c*). The result was recorded at $E_l = 9$ J, $\Delta = 0$ μm, $p = 15$ mm Hg. The conic shock wave localized near the axis of the focused laser beam (Fig. 4*c*) transforms at the later stage, at $t = 65$ ns, into a projection beyond the spherical shock wave (Fig. 4*e*). The structure of the projection is similar to that of the above-mentioned aneurisms.[7] Consequently, at least some class of aneurisms is the late stage of evolution of conic shock waves, and it should not be considered as a result of instability of spherical shock waves.

In some experiments the intensity distribution was smoothed with phase plates.[9] The ratio of the intensity drop in the focal spot to the mean level did not exceed 3%, and the size of the light spot in this case increased up to 140 μm, while the power density decreased down to $8 \cdot 10^{13}$ W/cm^2. As this took pace, no conic shock waves were observed beyond the cone bounded by the edge laser rays. Thus, the appearance of the conic shock waves is not directly connected with the inhomogeneous intensity distribution in the heating beam. At a relatively low power density ($q \approx 10^{14}$ W/cm^2), the waves localized near the laser beam axis arise. The increase of q up to approximately 10^{17} W/cm^2 leads to formation of several conic shock waves, whose axes can be oriented at a large angle to the axis of the focused laser beam.

In this study, we did not aimed at determining the cause of the appearance of the conic shock waves. Possibly, they are formed due to the transit of fast particles mentioned in Ref. 6. The result shown in Fig. 4*e* indirectly supports this assumption. The experiment was conducted at the following parameters: $E_l = 10$ J, $\Delta = 0$ μm, $p = 15$ mm Hg, $q = 2.6 \cdot 10^{16}$ W/cm^2, $t = 5$ ns. The conic shock wave has a markedly curved shape within the area of the impact-compressed gas and is similar to the trajectory of charged particles in the magnetic field, which, as known, is spontaneously generated in an inhomogeneous laser plasma and can reach significant values.[11]

In the area behind the front of a spherical shock wave, the zone with high-level inhomogeneity is observed near the "base" of every conic shock wave. In the interferograms, it manifests itself as dark areas having a complex spatial shape. Omitting the experimental details, let us note that darkening is indicative of a significant gradient of the refractive index in these zones, what results in refraction of rays in the sensing beam by the angle exceeding the aperture of the reproduction objective *15* (see Fig. 1).

Analysis of the experimental data shows that such inhomogeneity zones are directly connected with the above-mentioned peculiarities of the shock waves. Thus, the inhomogeneity in the impact-compressed gas (shown by a circle in Fig. 4*a*) leads to formation of a marked projection (shown by a circle in Fig. 4*b*) ahead of the front of the spherical shock wave at the late stage of evolution ($t = 65$ ns). The inhomogeneity having similar structure (shown by a circle in Fig. 4*d*) accompanies the appearance of a conic shock wave. The strongest conic shock waves localized near the axis of the heating laser beam correspond to better developed zones of inhomogeneity behind the front of a spherical shock wave.

Both the inhomogeneity zones and the front of the spherical shock wave introduce distortions of the screw type dislocations in the sensing beam. In the interferograms with a reference beam, such areas are seen as splitting of the interference fringes and are the result of transformations of the initially smooth coherent wave into a complex topologic object containing local spiral areas.[12] Note that similar structures appear in speckle-distorted fields as laser beams propagate through the turbulent atmosphere.

Thus, in this paper it is shown that as the plasma initiated by a Nd laser radiation with the subnanosecond pulse duration and the power density of $(8 \cdot 10^{13}$–$8 \cdot 10^{16})$ W/cm^2 on the surface of an object spreads into the residual gas, the conic shock waves, along with the spherical ones, are formed inside and outside the area occupied by laser beams. Consequently, the appearance of the shock waves is not directly connected with the inhomogeneous heating of the gas by a laser beam. However, at formation of the smooth intensity distribution in the heating laser beam the conic shock waves are localized mostly near the beam axis. At a late stage of the wave evolution, the spherical wave front acquires a complex shape: projections ahead of the main spherical shock wave are observed. With the use of a multiframe interferometer, it was shown that some of these projections are the late stage of evolution of the conic shock waves, and they should not be considered as a manifestation of unstable dynamics of the spherical shock waves.

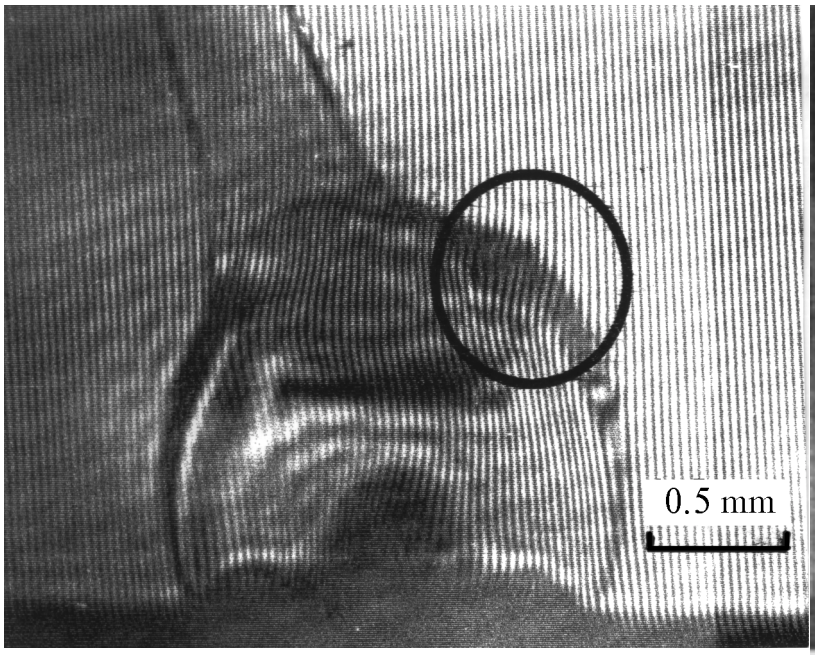

a

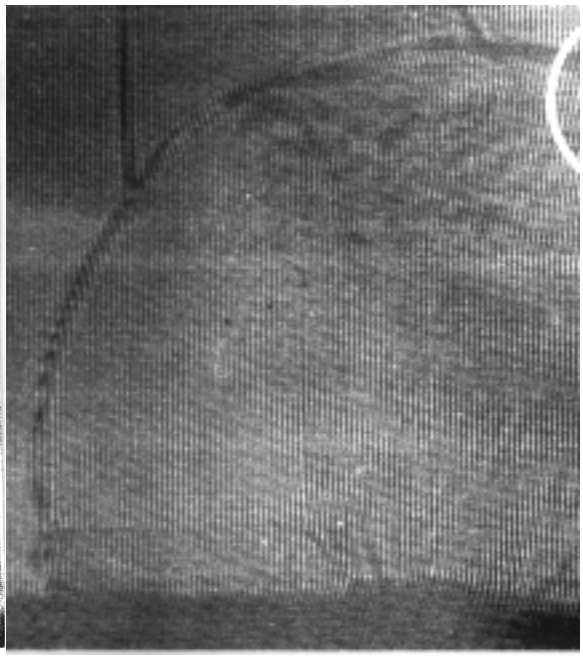

b

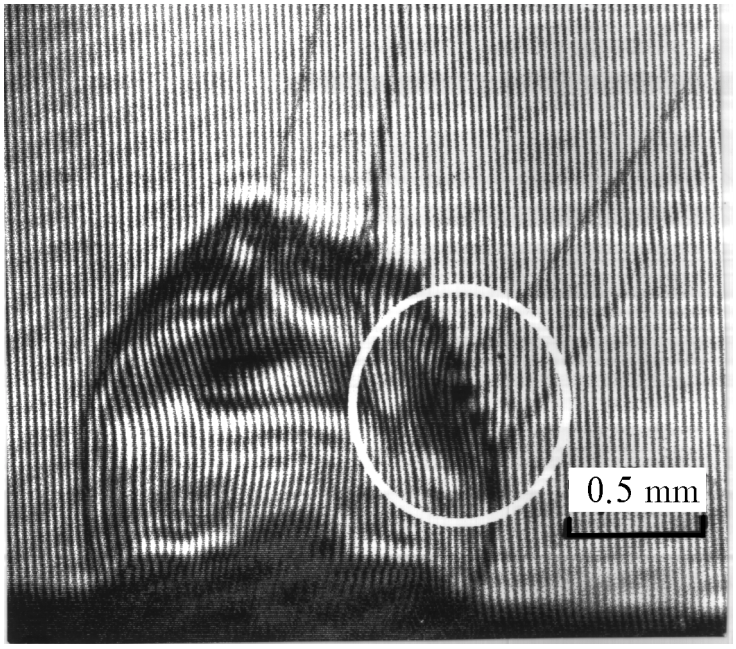

c

d

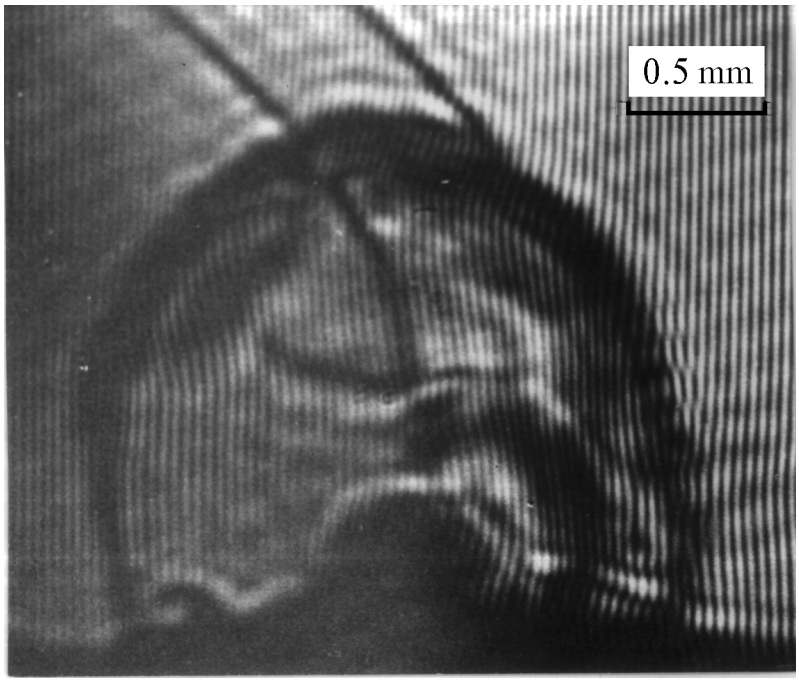

e

Fig. 4. Interferograms of shock waves: $q = 8 \cdot 10^{13}$ W/cm^2 (*b*); $q = 8 \cdot 10^{16}$ W/cm^2, $t = 5$ (*c*) and 65 ns (*d*); $q = 2.6$ (*e*).

References

1. N.N. Zorev, G.V. Sklizkov, and A.S. Shikanov, Zh. Eksp. Teor. Fiz. **82**, No. 4, 1104–1113 (1982).
2. O.B. Anan'in, Yu.A. Bykovskii, E.L. Stupitskii, et al., Kvant. Elektron. **14**, No. 11, 2313–2316 (1987).
3. O.B. Anan'in, Yu.A. Bykovskii, Yu.V. Eremin, et al., Kvant. Elektron. **18**, No. 7, 869–872 (1991).
4. N.N. Zorev, G.V. Sklizkov, and A.S. Shikanov, Pis'ma Zh. Eksp. Teor. Fiz. **38**, No. 9, 421 – 424 (1983).
5. B.L. Vasin, A.A. Erokhin, N.N. Zorev, et al., Trudy Fiz. Inst. Akad. Nauk **133**, 51 – 145 (1983).
6. N.G. Basov, Yu.A. Zakharenkov, N.N. Zorev, et al., "*Heating and compression of thermonuclear targets illuminated by laser*," in: Itogi Nauki i Tekhniki, Ser. Radiotekhnika (VINITI, Moscow, 1982), Vol. 26, 304 pp.
7. J.A. Stamper and B.H. Ripin, Phys. Fluids **31**, No. 11, 3353–3361 (1988).
8. V.N. Alekseev, E.G. Bordachev, V.G. Borodin, et al., Izv. Akad. Nauk SSSR, Ser. Fizika **48**, No. 8, 1477–1484 (1984).
9. V.G. Borodin, V.A. Gorbunov, S.S. Gulidov, et al., Izv. Akad. Nauk SSSR, Ser. Fizika **53**, No. 8, 1467–1473 (1989).
10. V.G. Borodin, S.V. Krasov, A.N. Shatsev, et al., Opt. Zh., No. 12, 33–38 (1996).
11. A.V. Gurvich, Zh. Eksp. Teor. Fiz. **74**, 539–552 (1978).
12. B.D. Bobrov, Kvant. Elektron. **18**, No. 7, 886–890 (1991).